Enhanced Composite Patch Repair for Cracked Plates Through Genetic Algorithm Optimization

KACEMI Nadjib[1], YAHIAOUI Reda[1]

[1] *Lab of Industrial Production and Maintenance Engineering, Institute of Maintenance and Industrial Safety, University of Oran2 Mohamed Ben Ahmed; P.B 1015 El M'naouer 31000 Oran Algeria*

E-mail: kacemi.nadjib@univ-oran2.dz, reda.yahiaoui@univ-oran2.dz.

Abstract: bonded composite patch repair technology has gained widespread adoption across industries such aerospace, wind energy, and various industrial sectors due to its cost-effectiveness, versatile design, and lightweight characteristics. This technique effectively reduces the stress intensity factor SIF at the crack tip, thereby inhibiting crack propagation and prolonging the structural lifetime. However, the application of composite patches without optimization of their shape, size and properties can result suboptimal repairs, compromising the structural integrity and safety. In this study, we investigate the influence of the dimensions of a rectangular composite patch on the SIF the crack tip, an essential parameter for assessing the repair's effectiveness. Using the finite element method FEM analysis, we developed a model that integrates FEM with bio-inspired optimization technique, specifically a genetic algorithm GA, to optimize the length and the width of the composite patch for SIF reduction. The results demonstrate that the model employing the GA effectively identifies the optimal dimensions for composite patch repairs, enhancing their efficiency.

Keywords: genetic algorithm, stress intensity factor, composite patch, finite element method, optimization. metaheuristic.

1. INTRODUCTION

Structural damages such as cracks, delamination and notches are inevitable occurrences throughout the service life of engineering structure, often resulting from fatigue, corrosion, and accidents (Mall & Conley, 2009), (Aabid et al., 2020). Over the decades, extensive search has focused on repairing such damages. Among the technics explored, bonded composite patch has emerged as a prominent solution due to its efficacy in reducing stress at the crack tip (Ahn et al., 2010). This method offers significant advantages over traditional repair techniques such as riveting, fastening, or stop-hole drilling (Khan & Essaheb, 2017).

Research into crack propagation and repair methods within composite has been substantial. M. Alpesh et al. (Makwana et al., 2018) conducted a three dimensional numerical investigation to examine the effects of both symmetric and asymmetric composite patches on the induced SIF at the crack tip. Similarly, K. Sadek et al. (Sadek et al., 2018) performed a comprehensive numerical analysis to investigate crack propagation in bonded composite, evaluating various composite shapes for repair applications. M. Berrahou et al. (Mohamed & Khaoula, 2022) also contributed with a numerical study on repairing notched cracked in composites using composite patches.

To assess the effectiveness of bonded composite patch repairs, various approaches including analytical, numerical and experimental methods have been employed (Aabid, 2023), (Gorawade et al., 2023), (Makwana et al., 2018), (Li et al., 2020). The SIF is a crucial criterion for evaluating repair efficacy, as high SIF values accelerate crack propagation and compromises structural integrity. Thus, minimizing the SIF at the crack tip is crucial for ensuring effective repair operations. Researchers have explored various methodologies to minimize the SIF through the optimization of patch geometry. B. Matias et al. (Braun et al., 2018) persuade this goal by using a topological optimization algorithm to derive the optimal composite patch design. Concurrently, A. Abdul (Aabid, 2023) utilized analytical modelling and Taguchi design principles to minimize the SIF. D. Bash et al. (Do & Lenwari, 2020) combined genetic algorithms with genetic programing techniques to achieve an optimal patch design that effectively mitigates the SIF while minimizing the patch volume. Additionally, E. Leonel et al. (Echer et al., 2021) conducted a comprehensive study on optimizing conventional repair geometries, focusing on rectangular and elliptical configurations.

The efficacy of bonded repairs is influenced by composite material selection, as well as patch geometry, which plays a crucial rule in SIF minimization. Consequently, determining the optimal length and width of composite patch present a significant challenge. The present study aims to optimize patch dimensions using genetic algorithm (GA), an artificial intelligence search metaheuristic inspired by biological evolution process, including inheritance, mutation, selection, and crossover (Tabassum, 2014).

2. Numerical study

2.1. Geometry and materials

The geometry of the studied structure is presented in figure 1, where a thin steel plate containing a central crack is bonded with a double side rectangular composite patch. The adhesive material used to join the cracked plate with the composite patch is the FM -73. The properties of the used materials are summarized in table 1.

Table 1: material properties of cracked plate, adhesive layer and composite patch

Properties	Steel	Boron/ epoxy	FM 73 adhesive
Longitudinal modulus, E_1 (GPa)	200	208	1.1
Transverse in-plane modulus E_2 (GPa)	-	25.4	-
Transverse out-of-plane modulus E_3 (GPa)	-	25.4	-
In plane shear modulus, G_{12} (GPa)	-	7.2	0.382
Out-of-plane shear modulus, G_{13} (GPa)	-	7.2	-
Out-of-plane shear modulus, G_{23} (GPa)	-	4.9	-
Major in-plane poison's ratio, υ_{12}	0.33	0.1677	0.44
Major out-of-plane poison's ratio, υ_{13}	-	0.1677	-
Major out-of-plane poison's ratio, υ_{23}	-	0.36	-

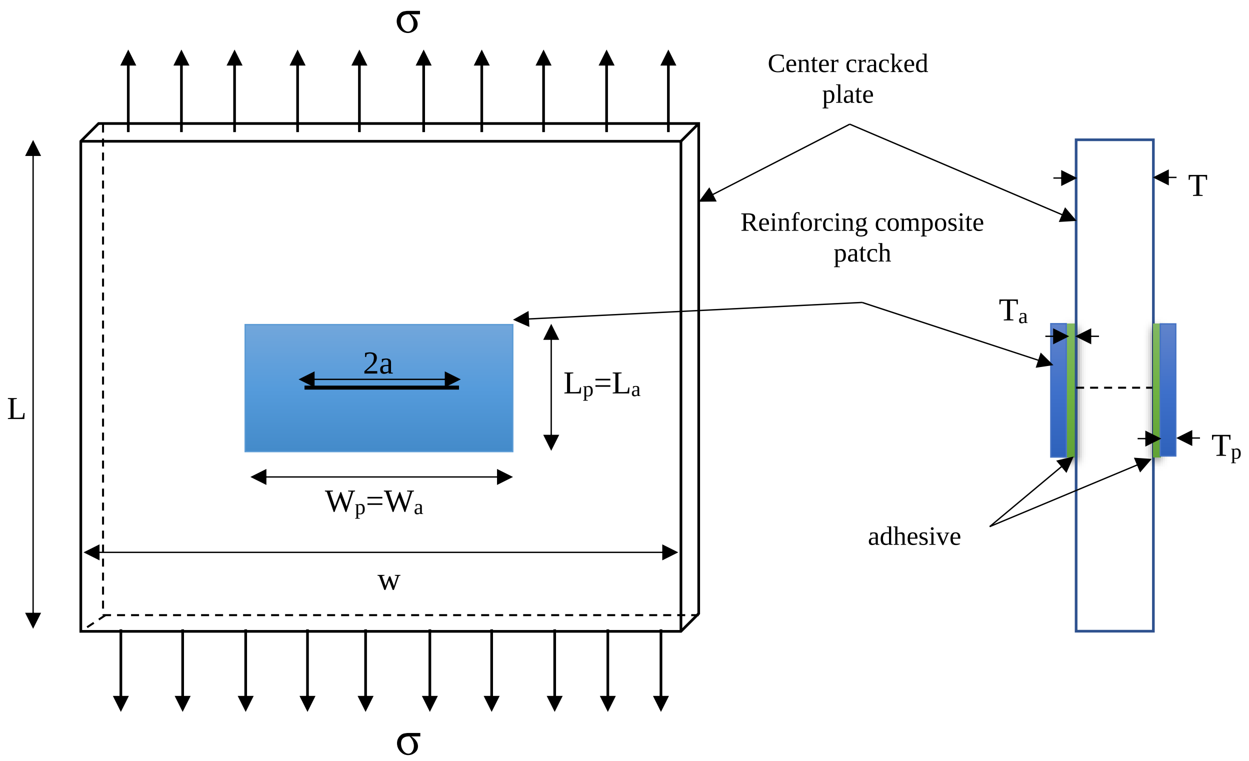

Figure 1. geometrical model of the cracked plate with double sided patch

The steel plate has a length (L) of 720 mm, a width (W) of 720 mm, a thickness (T) of 1.6 mm, and a pre-existent crack of length $2a$ = 72 mm. The adhesive and the patch are denoted using subscripts a and p, respectively. The thickness of the adhesive (T_a) is 0.2 mm and the thickness of the patch (T_p) is 0.6 mm.

2.2. Finite element analysis

The analytical solution of a center cracked plate (Tada et al.,1973), without repair, was used to evaluate the SIF :

$$K_I = F(\frac{a}{w})\sigma\sqrt{\pi a} \quad (1)$$

Where σ is the applied normal stress, a is the half of the crack length and $F(a/w)$ is a dimensionless quantity that depends on the cracked plate geometry, the type of loading and the ratio of the crack length to the plate width ($\frac{a}{w}$), which is defined as:

$$F\left(\frac{a}{w}\right) = \{1 - 0.025\left(\frac{a}{w}\right)^2 + 0.06\left(\frac{a}{w}\right)^4\}\sqrt{sec\frac{\pi a}{2w}} \quad (2)$$

On the other hand, for the FEM analysis, Hex-dominated elements were used to mesh the entire plate, with the exception of the crack tip. Due to its sharp geometry, wedge elements were employed at the crack tip, figure 2-a. Considering the

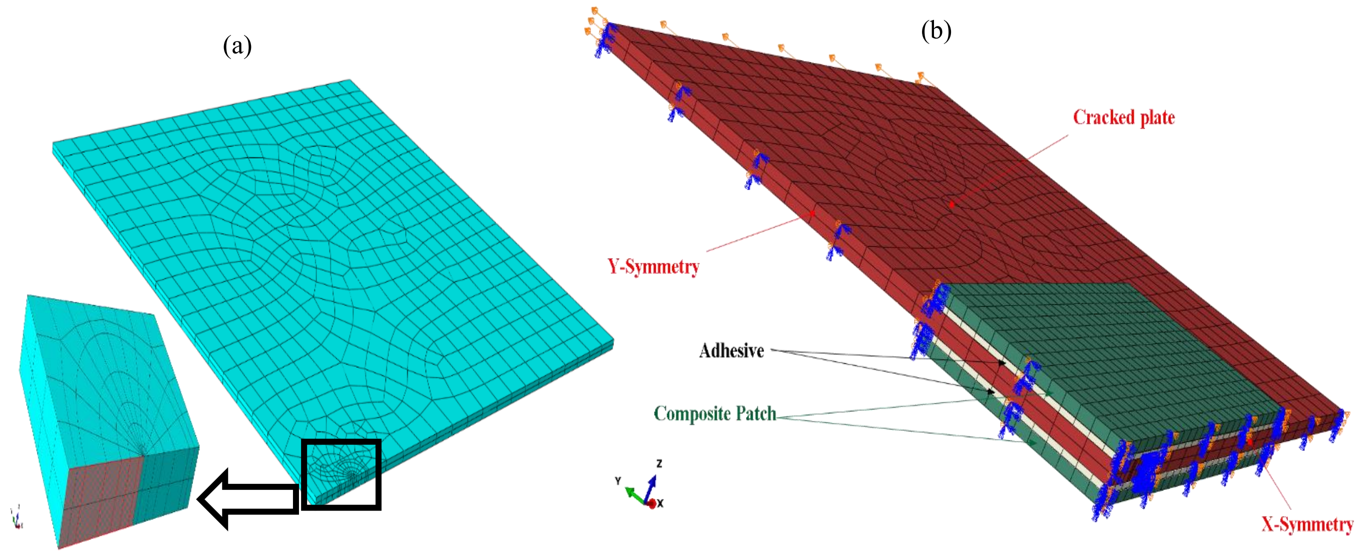

Figure 2. Representation of meshed cracked plate (a) and repaired plate mesh with load and boundary conditions (b).

symmetry of the model, only a quarter of it was used in the analysis. However, Hex elements were used to mesh both the adhesive and the composite patch, figure 2-b.

The obtained value of SIF (552.4 MPa.$\sqrt{mm}$) for an applied stress of 50 MPa is in good agreement with the analytical solution (534.91 MPa.$\sqrt{mm}$) provided by (Tada et al.,1973), where only an error of 3.27% is observed.

2.3. effect of patch length and width on SIF

to investigate the effect of patch width and length on the resulting SIF at the crack tip, one parameter (either width or length) is fixed at 180 mm while the other parameter is varied.

2.3.1. effect of patch length

Figure 3 illustrates the effect of patch length on the SIF, where the SIF is significantly influenced by the length of the patch. It reaches its lowest value when the ratio $(\frac{L_p}{2a})$ is approximately 1.5. Notably, the variation in SIF with respect to $(\frac{L_p}{2a})$ exhibits a two-stage pattern: an initial stage with a significant decrease in SIF values, followed by a second stage where the SIF increases as the $(\frac{L_p}{2a})$ ratio continues to rise. The increase and decrease of the SIF can be described by a linear relationship.

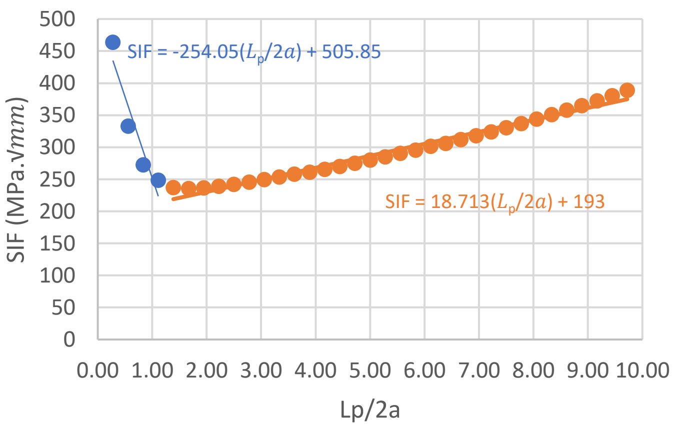

Figure 3. Effect of $(\frac{L_p}{2a})$ on the stress intensity factor.

2.3.2. effect of patch width

The effect of patch width on the SIF value is less pronounced than that of the length patch. Figure 4 illustrates that, with an increase of $(\frac{W_p}{2a})$, there is a global linear decrease in the SIF value.

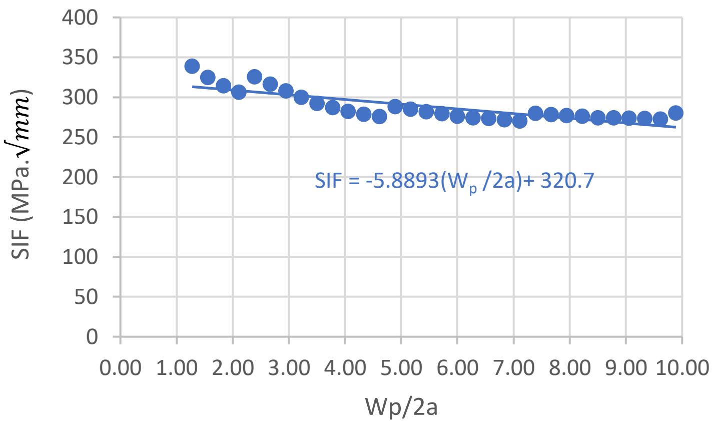

Figure 4. Effect of $(\frac{W_p}{2a})$ on the stress intensity factor.

3. Genetic Algorithm for Optimizing Patch Dimensions

A genetic algorithm has been developed to optimize the dimensions of the patch by concurrently adjusting its length and width. Thus, the SIF value was computed, for each pair of patch length and width, through FEM analysis. The process begins with the random generation of an initial population comprising diverse sets of patch width and length. Each individual in this population represents a potential solution for the patch dimensions. In this study, the population size is set

to 40 individuals, with patch width ranging from 46 – 360 mm and patch length from 10 – 360 mm.
On the other hand, an objective function is selected to quantify the design performance, typically based on minimizing the SIF. This function is computed for each individual within the initial population, allowing the determination of their efficacy. Individuals exhibiting superior performance, as evaluated by the objective function, are identified. Following the assessment of fitness for each individual, the two individuals displaying optimal performance concerning the selective objective function are chosen as parents. These parents will contribute genetic material to generate the next population.
Utilizing genetic concepts such as crossover and elitism, a new population (offspring) is generated from these parents. The decision regarding the individuals subjected to the crossover operator and those to the elitism operator is crucial. A genetic information is exchanged among selected individuals to create new offspring. The genetic material of individuals exhibiting favorable traits is preserved through the elitism operation, transferring them to the new population without alteration.
To effectively explore a design space of larger dimensions and prevent premature convergence, the mutation concept is employed. Random mutations are introduced to some individuals in the newly generated population, leading to partial modifications in their parameter values. This enhances the algorithm's capacity to traverse expansive design landscape comprehensively.
The algorithm iteratives through multiple generations, typically a predefined number of 30 in our study, resulting in total of 1200 simulations. During each generation, individuals from the population are selected for reproduction based on their fitness scores, facilitating the exploration of the solution space. The iterative process aims to identify the optimal patch dimensions that minimize the SIF.
By iteratively applying selection, reproduction, and mutation operations, the GA explores and refines potential solutions, figure 5, ultimately converging towards an optimal set of patch dimensions that fulfill the design objectives.

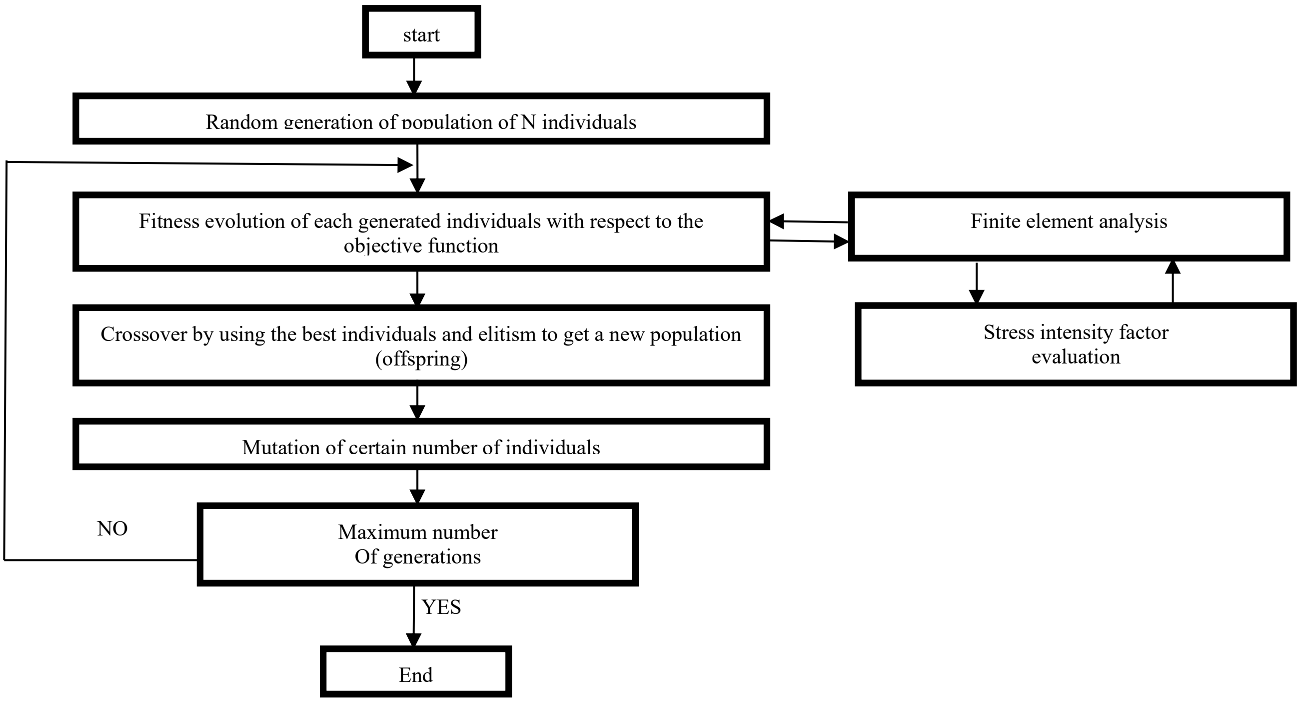

Figure 5. flow-chart of GA implemented in FEM code applied to the dimension's optimization of a patch repair.

Figure 6-a illustrates the influence of composite patch dimensions on the SIF and the dispersion of potential solutions derived from the objective function via genetic algorithm analysis. It is evident that the SIF escalates proportionally. The optimal solution identified by the GA yields an SIF value of 231.8 $MPa.\sqrt{mm}$ with patch dimensions of 228.5 mm in width and 63.6 mm in length.
In figure 6b, a contour plot illustrating the SIF in relation to the ratios ($\frac{Wp}{2a}$) and ($\frac{Lp}{2a}$) is presented. This visualization underscores the notable influence exerted by these ratios on the SIF. Notably, it becomes apparent that low levels of SIF occur within specific intervals: (1 to 3) for the ($\frac{Lp}{2a}$) ratio and (4 to 10) for the ($\frac{Wp}{2a}$) ratio. Deviation from these intervals results in a marked increase in SIF values. This observation underscores the significance of maintaining these ratios within prescribed bounds to mitigate SIF-induced structural concerns effectively.
Figure 7 illustrates the optimization process, portraying the progressive evolution of the minimum value of the stress intensity factor alongside the number of generations within the GA. It is noteworthy that a discernible trend emerges, wherein the SIF demonstrates a decremental pattern as a generation number increases, indicating an inverse relationship between the SIF and the generation count.

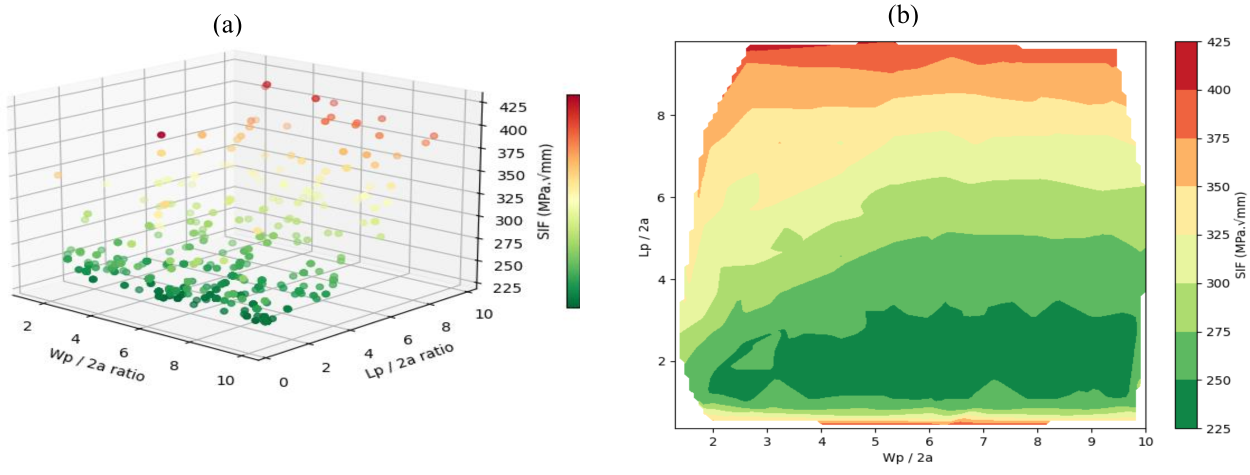

Figure 6. Individuals' distribution in optimization search domain (a), contour plot SIF vs $\left(\frac{W_p}{2a}\right)$ and $\left(\frac{L_p}{2a}\right)$ (b).

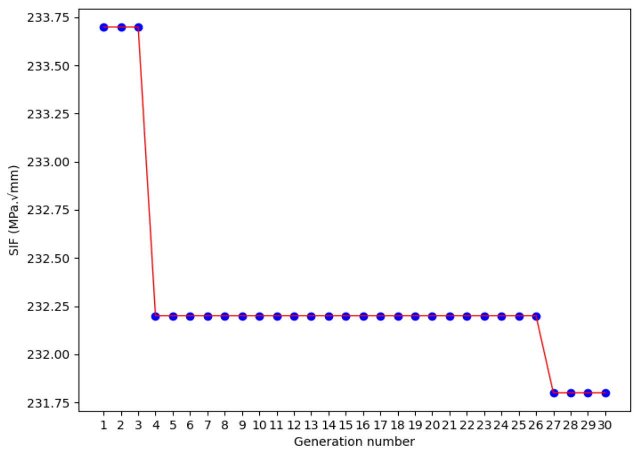

Figure 7. global best SIF evolution with generation number

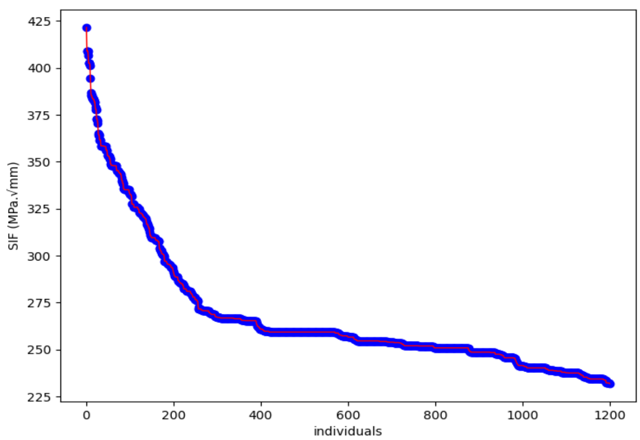

Figure 8. SIF with respect to number of individuals

Figure 8 illustrates the variation of SIF across the spectrum of solutions explored within the search domain. Noteworthy is the substantial range observed, extending from the global worst solution at 421.6 $MPa.\sqrt{mm}$ to the global best solution at 231.8 $MPa.\sqrt{mm}$. This wide span underscore the efficacy of the GA in conducting an exhaustive search for the optimal solution. Specifically, the traversed over 200 individuals characterized by unfavorable SIF values, while also scrutinizing more than 1000 individuals exhibiting favorable SIF values. This concerted effort highlights the GA's strategic focus on the domain housing the minimum solution, thereby exemplifying its robust search capabilities.

4. Conclusion

The finite element method was employed to evaluate the stress intensity factor at the crack tip of the repaired plate. By applying a genetic algorithm to minimize the SIF through the identification of the optimal configuration of patch width and length, the following conclusions were drawn:

- The dimensions of the composite patch play a crucial role in the repair of cracked structures. If the patch is not adequately sized, it can lead to high stress intensity factors at the crack tip.
- Optimizing the patch size cannot be successfully carried out by evaluating the effect of each dimension separately.
- The GA algorithm can be effectively applied in determining the optimum size of the composite patch

REFERENCES

Aabid, A. (2023). Optimization of Reinforcing Patch Effects on Cracked Plates Using Analytical Modeling and Taguchi Design. Materials, 16(12). https://doi.org/10.3390/ma16124348

Aabid, A., Hrairi, M., & Mohamed Ali, J. S. (2020). Optimization of composite patch repair for center-cracked rectangular plate using design of experiments method. Materials Today: Proceedings, 27, 1713–1719. https://doi.org/10.1016/j.matpr.2020.03.639

Ahn, J. S., Basu, P. K., & Woo, K. S. (2010). Analysis of cracked aluminum plates with one-sided patch repair using p-convergent layered model. Finite Elements in Analysis and Design, 46(5), 438–448. https://doi.org/10.1016/j.finel.2010.01.008

Braun, M., Villa, E. I., Riojas-Roldán, H., & Rocco, C. G. (2018). A topological optimization algorithm applied to the design of composites patch repair of mixed-mode cracked plate. Journal of Composite Materials, 52(17), 2387–2395. https://doi.org/10.1177/0021998317745587

Do, B., & Lenwari, A. (2020). Optimization of Fiber-Reinforced Polymer Patches for Repairing Fatigue Cracks in Steel Plates Using a Genetic Algorithm. Journal of Composites for Construction, 24(2), 1–15. https://doi.org/10.1061/(asce)cc.1943-5614.0001005

Echer, L., de Souza, C. E., & Marczak, R. J. (2021). A study on the best conventional shapes for composite repair patches. Materials Research, 24, 1–8. https://doi.org/10.1590/1980-5373-MR-2021-0304

Gorawade, A., Nimje, S. V., & Khode, A. (2023). Numerical analysis of cracked aluminium panel repaired with functionally graded adhesively bonded patch. Materials Today: Proceedings, 72, 1467–1470. https://doi.org/10.1016/j.matpr.2022.09.347

Tada, H., Paris, P. C., & Irwin, G. R. (1973). The stress analysis of cracks. Handbook, Del Research Corporation, 34(1973).

Khan, S. M. A., & Essaheb, M. (2017). Effect of Patch Thickness on the Repair Performance of Bonded Composite Repair in Cracked Aluminum Plate. Materials Today: Proceedings, 4(8), 9020–9028. https://doi.org/10.1016/j.matpr.2017.07.255

Li, Z., Jiang, X., Hopman, H., Zhu, L., & Liu, Z. (2020). External surface cracked o ff shore steel pipes reinforced with composite repair system subjected to cyclic bending : An experimental investigation. Theoretical and Applied Fracture Mechanics, 109(June), 102703. https://doi.org/10.1016/j.tafmec.2020.102703

Makwana, A., Shaikh, A. A., Bakare, A. K., & Saikrishna, C. (2018). 3D Numerical Investigation of Aluminum 2024-T3 Plate Repaired with Asymmetric and Symmetric Composite Patch. Materials Today: Proceedings, 5(11), 23638–23647. https://doi.org/10.1016/j.matpr.2018.10.153

Mall, S., & Conley, D. S. (2009). Modeling and validation of composite patch repair to cracked thick and thin metallic panels. Composites Part A: Applied Science and Manufacturing, 40(9), 1331–1339. https://doi.org/10.1016/j.compositesa.2008.08.007

Mohamed, B., & Khaoula, A. (2022). Numerical analysis of the repair performance of Notched Cracked Composite Structure repaired by composite patch A R T I C L E I N F O. Journal of Materials and Engineering Structures, 9, 317–326.

Sadek, K., Aour, B., Bachir Bouiadjra, B. A., Fari Bouanani, M., & Khelil, F. (2018). Analysis of crack propagation by bonded composite for different patch shapes repairs in marine structures: A numerical analysis. International Journal of Engineering Research in Africa, 35, 175–184. https://doi.org/10.4028/www.scientific.net/JERA.35.175

Tabassum, M. (2014). a Genetic Algorithm Analysis Towards Optimization Solutions. International Journal of Digital Information and Wireless Communications, 4(1), 124–142. https://doi.org/10.17781/p001091